Fixed Bed Adsorption Drying

C. W. CHI and D. T. WASAN

Institute of Gas Technology and Illinois Institute of Technology, Chicago, Illinois

In this paper, mathematical models for a single adsorbate component present in a gas phase have been developed for isothermal and adiabatic dynamic adsorption-desorption processes with special emphasis on adsorption drying by supported hygroscopic salts. The proposed generalized models are applicable to both an unsupported absorbent bed and a fixed bed of adsorbents impregnated on a supporter which may have nonlinear equilibrium relationships. The partial differential equations governing the dynamic adsorption-desorption processes and the nonlinear equilibrium relations were solved numerically on the digital computer.

An experimental study was conducted to measure the adsorption and desorption rates of water vapor by lithium chloride impregnated on a solid supporter, Torvex.

The proposed adiabatic adsorption-desorption model has been verified for unsupported adsorbent beds in the cases of water vapor adsorption from air by silica gel and of methane adsorption from a helium-methane mixture by activated carbon. The validity of the generalized adiabatic model for supported adsorbent beds with nonlinear equilibrium relationships was established by a direct comparison of experimental data obtained in this study with the predicted values.

The major applications of adsorption methods have been in the field of air and gas drying and solvent recovery. Adsorption drying has been competitive for a number of applications because it has many advantages over other methods, particularly when a high degree of moisture removal is required.

An extensive literature search (*9*) disclosed that neither data nor adequate models have been presented for the dynamic dehydration in a fixed bed of supported adsorbents, despite, the fact that such a method is commercially well-developed and its potential application for adsorption refrigeration has been recognized.

The present study is concerned with the adsorption drying of air by hygroscopic salts impregnated on a supporter and the regeneration of adsorbents by a flow of hot air. The performance during the adsorption portion of the cycle employing an unsupported absorbent bed has been the subject of considerable interest. However, no work has been done on the reactivation of adsorbents, supported or unsupported. The regeneration of an adsorber prior to its use is equally important in a cyclic process since its subsequent performance during adsorption is essentially dependent upon the thoroughness of the regeneration process and the thermal state of adsorbent bed.

The objectives of this study are twofold: to develop the isothermal and adiabatic adsorption-desorption models for both an unsupported adsorbent bed and a fixed bed of adsorbents impregnated on a supported bed which may have nonlinear equilibrium relationships, and to verify the proposed models by a direct comparison of experimental data with the predicted values at simulated experimental conditions for design purposes.

In an effort to clarify the general problem and demonstrate an application of the models presented, special attention is given to the water adsorption and desorption from air by lithium chloride impregnated on a supporter, Torvex. An elaborate experimental study was conducted to measure the adsorption-desorption rates. The approach used and the experimental technique are detailed elsewhere (*9*).

THEORETICAL ANALYSIS

Isothermal Adsorption-Desorption Analysis

Isothermal dynamic adsorption, by definition, precludes heat effects, so the analysis is based on the material balance and the equilibrium relationship between the adsorbate in the gas and in the adsorbent.

The isothermal adsorption of water vapor from a mixture with an inert fluid has been treated by Hougen and Marshall (*17*), Gamson, et al. (*14*), Michaels (*22*), Treybal (*35*), Eagleton and Bliss (*11*), Vermeulen and Hiester (*37*), Vermeulen (*38*), Rosen (*26, 27*), Testin (*30*), Thomas (*32*), Tien and Thodos (*34*), and Fosberg (*13*). Similar problems in heat transfer associated with certain types of regenerators and preheaters have been solved by Anzelius (*2*), Nusselt (*24*), Schumann (*28*), Hausen (*16*), and Brinkley (*5*).

With exception of Thomas (*32*), Vermeulen and Hiester (*37*), and Fosberg (*13*), all other investigators assumed a linear adsorption isotherm. The solutions of Thomas and Vermeulen and Hiester are applicable to specific cases of nonlinear systems, that is at constant separation factor. Recently Fosberg (*13*), obtained the solution with an analog computer for nonlinear isotherm.

C. W. Chi is presently with the W. R. Grace and Co., Washington Research Center, Clarksville, Maryland.

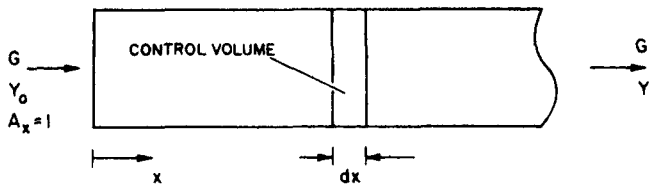

Fig. 1. Schematic of control volume for adsorption analysis.

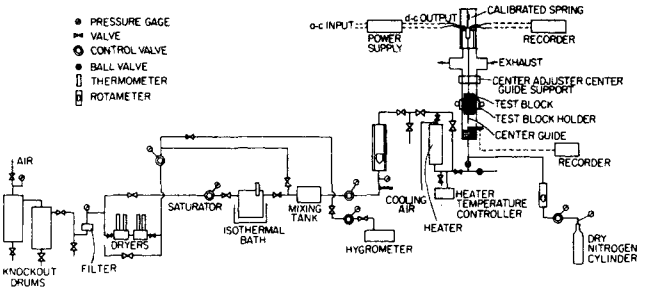

Fig. 2. Schematic of rate apparatus.

In this study, the digital computer solution is sought for any equilibrium relationship for both supported and unsupported adsorbent beds by extending the Hougen-Marshall Model.

The application of the Hougen-Marshall Model to the isothermal dynamic adsorption processes encounters several difficulties. First, assumption of a linear equilibrium between the adsorbate in the gas phase and in the adsorbent does not hold for many systems of interest. Second, Hougen and Marshall and other investigators failed to demonstrate how their solutions could be applied to systems where the adsorbent is coated on a supporter, which is the kind of system presently of interest.

To overcome these shortcomings, an attempt was made to develop a more generalized method of analysis. In the following section the Hougen-Marshall model was extended to include the isothermal adsorption process for any equilibrium relationship.

Fundamental equations for the present model have been derived relaxing all the assumptions of Hougen and Marshall except for the two, that is, the overall resistance to mass transfer is the sum of the diffusional resistances in the gas phase and the solid phase, and that the overall driving force is linear. Furthermore, in the subsequent development it is necessarily assumed that the adsorbent is uniformly impregnated on the supporter.

Fundamental Equations for the Present Isothermal Model

Referring to the control volume shown in Figure 1 the material balances on the adsorbate yield

$$\rho F \left(\frac{\partial Y}{\partial t}\right)_x + G \left(\frac{\partial Y}{\partial x}\right)_t = -\rho_s \alpha \left(\frac{\partial w}{\partial t}\right)_x \quad (1)$$

$$\rho_s \alpha \left(\frac{\partial w}{\partial t}\right)_x = K_Y a_v (Y - Y^*) \quad (2)$$

where

$$Y^* = f(w) \quad (3)$$

with the initial and boundary conditions,

$$w(x, t^0) = w^0 \quad (4)$$

$$Y(0, t) = Y_0 \quad (5)$$

Defining n and τ by

$$n = \frac{K_Y a_v x}{G} \quad (6)$$

$$\tau = \frac{K_Y a_v}{\rho_s \alpha} \left(t - \frac{\rho F x}{G}\right) \quad (7)$$

transforms $Y(x, t)$ and $w(x, t)$ into the new coordinate system $Y(n, \tau)$ and $w(n, \tau)$:

$$\left(\frac{\partial Y}{\partial n}\right)_\tau = -(Y - Y^*) \quad (8)$$

$$\left(\frac{\partial w}{\partial \tau}\right)_n = (Y - Y^*) \quad (9)$$

$$Y^* = f(w) \quad (10)$$

$$w(n, 0) = w^0 \quad (11)$$

$$Y(0, \tau) = Y_0 \quad (12)$$

This set of equations and the initial and the boundary conditions define the adsorption process. The following numerical methods were adopted to obtain the solutions of these equations.

Numerical Methods

The numerical technique employed here was that suggested by Acrivos (*1*) and closely follows Bullock's approach (*7*).

The system of differential equations was solved by the modified Euler method (23) and the predictor-corrector method (*4*).

To establish the accuracy and the validity of the numerical technique, the Anzelius equations were first solved on a digital computer. The numerical results obtained were compared with the Anzelius' analytical solutions (*2*). The agreements were found to be excellent (*9*).

After some confidence was established in the numerical method, the system of differential Equations (8) and (9) with initial and boundary conditions (11) and (12) and a nonlinear equilibrium relationship (10) was solved both for silica gel and for lithium chloride impregnated on a solid supporter. A summary of the computer runs is listed elsewhere (*9*).

These results indicated that a substantial error will be introduced if the effect of the supporter is neglected. It is to be pointed out that the same analysis together with the present computer program can be used to obtain solutions for isothermal desorption cases with nonlinear equilibrium relations.

The general method of calculation can be applied to several systems of interest. In the case of single tube adsorbent the dimensionless variables n and τ become

$$n = \frac{2K_Y a_A x}{GR} \quad (13)$$

$$\tau = \frac{K_Y a_A}{\rho_s' \alpha (1 - F)\, \epsilon} \left(t - \frac{\rho F x}{u}\right) \quad (14)$$

and the solutions presented for fixed bed operation can be used directly.

ADIABATIC ADSORPTION-DESORPTION ANALYSIS

When water vapor is adsorbed by the desiccant, heat is released because the adsorption process is exothermic. It is difficult to maintain isothermal conditions, so in practice most adsorbent beds are operated adiabatically. Under adiabatic operation the heat released raises the temperature of the bed and this rise in temperature decreases the adsorption rate. Thus the analysis presented in the previous section for isothermal adsorption does not apply to most systems that operate nonisothermally. Even

if the exit stream temperatures remain nearly constant, the assumption that adsorption is isothermal is erroneous because the temperature of the mass transfer zone, rather than the inlet or outlet stream temperature, determines the adsorption rate. Therefore, the analysis should include the changes in enthalpy as well as the adsorbate concentrations in the gas and the adsorbent phases.

Hougen and Marshall (*17*) suggested a graphical method based upon Grossman's method for heat transfer for the adiabatic dynamic adsorption in gases flowing through granular beds. However, the graphical technique is tedious, costly, and impractical due to the small time interval and bed length increment required. Acrivos (*1*), Threlkeld (*33*), Van Arsdel (*36*) and Carter (*8*) developed models and presented numerical techniques for this problem.

Recently, Lee and Cummings (*19*) proposed a correlation between the experimental break capacity of a nonisothermal air drier with silica gel and that calculated from the analytical solution for isothermal conditions. The Lee-Cummings design method is applicable for systems whose equilibria can be linearized and when correlations are available. Collins (*10*) introduced the use of the LUB (equivalent length of unused bed) equilibrium section concept for design practice in sizing fixed-bed molecular sieve drying and purification systems. This empirical approach is useful when experimental data or correlations are available to predict the break capacity.

More recently Meyer and Weber (*20*) extended Rosen's model (*26, 27*) and obtained a numerical solution of the differential equations. The model incorporates heat and mass transfer resistances within and around the adsorbent particles. It is developed for packed beds of homogeneous spherical particles of uniform size. The governing differential equations, six in number, were solved numerically on a digital computer. The model was tested using a packed bed 2 in. in diameter and 60 in. deep with activated carbon. A methane-helium mixture was passed through the bed. Since no pore diffusivity correlations are available, the effective intraparticle diffusivity was determined by simulating the actual experiments on the digital computer and matching the observed and calculated effluent curves. Meyer's (*21*) data did not produce a consistent effective intraparticle diffusivity, but varied from 0.058 (2 runs) to 0.10 (1 run) for the limited range of operation. Consequently, the results of the experiment confirmation are inconclusive and the validity of the model is yet to be established by a crucial test.

There are several drawbacks in Meyer-Weber model: many of the adsorbent beds cannot be adequately approximated as spherical particles of uniform size; the solid diffusion coefficients are unknown but the solution of the model is sensitive to the intraparticle diffusivity and requires a high accuracy of the diffusivity determination while only the magnitude of the transfer coefficient can be evaluated by matching the experimental data and the numerical solutions; and the model is not applicable to fixed beds of hygroscopic salts impregnated on supporters that are of special interest in the present study.

Therefore effort has been directed to developing generalized models that describe the dynamic behavior of a fixed bed by applying the overall resistance—linear driving force concept. An assumption is made that the overall resistance to the mass transfer is the sum of the diffusional resistances in the gas and solid phases. Bullock (*6*) recently obtained the numerical solutions of the differential equations developed by Threlkeld (*33*) for a case of adsorption of water vapor by silica gel in a fixed bed. Bullock also confirmed the validity of the model by direct comparisons with the results of experiments. His

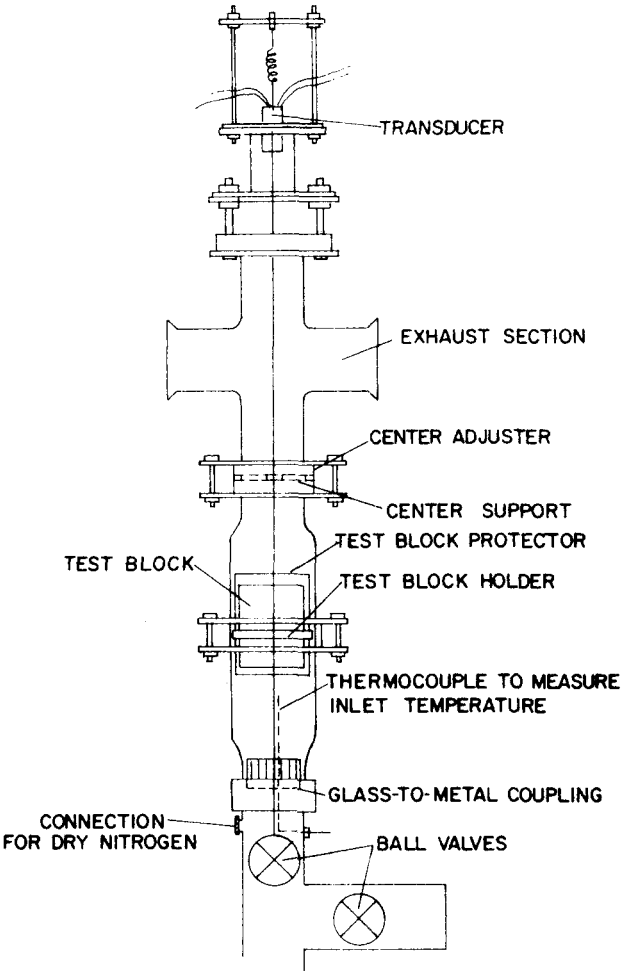

Fig. 3. Test section.

model, developed for a fixed bed of adsorbent, is not applicable when an adsorbent is impregnated on a supporter. It is to be noted that the Threlkeld-Bullock model (*7*) can be readily reduced from the generalized model which is presented next.

Derivation of Fundamental Equations for the Generalized Model for Adiabatic Adsorption

The behavior of a fixed bed adsorber is described if the concentrations and temperatures in the gas stream and

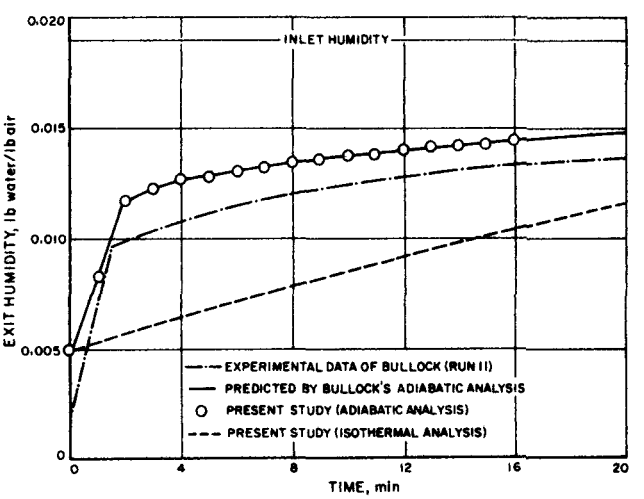

Fig. 4. Comparison of experimental and predicted exit humidity vs. time for silica gel (run 11).

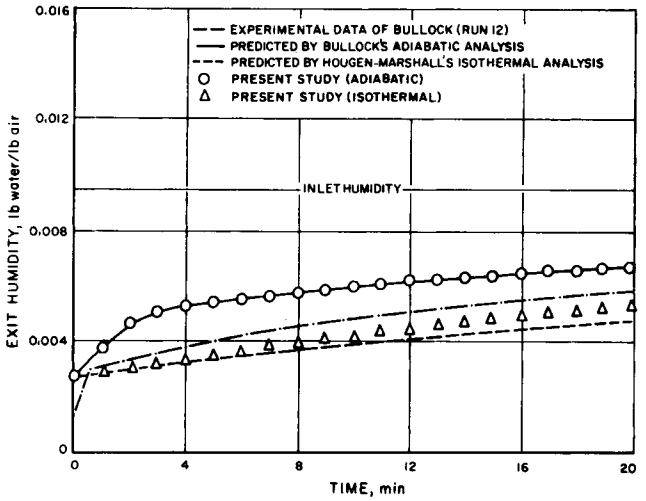

Fig. 5. Comparison of experimental and predicted exit humidity vs. time for silica gel (run 12).

in the solid phase are evaluated at any time and position in the bed. The equations required to evaluate these principal dependent variables were formulated from the laws of conservation of material and energy. The analysis developed in this section apply in general to the adiabatic adsorption and desorption of a single fluid from and to a mixture with an inert fluid.

Consider a flow of humid air through a freshly regenerated fixed bed of adsorbents or adsorbents coated on a supporter, as shown in Figure 1.

The generalized governing differential equations for the adiabatic dynamic adsorption process were derived under the same simplifying assumptions as in the case of isothermal analysis except that the adsorption takes place adiabatically; the flow is one dimensional, and that the heat and mass transfer coefficients are constant.

Referring to the control volume as shown in Figure 1 the material balances on the adsorbate in the gas and in the adsorbent are as follows:

$$\rho F\left(\frac{\partial Y}{\partial t}\right)_x + G\left(\frac{\partial Y}{\partial x}\right)_t = -\rho_s \alpha \left(\frac{\partial w}{\partial t}\right)_x \tag{15}$$

$$\rho_s \alpha \left(\frac{\partial w}{\partial t}\right)_x = K_Y a_v (Y - Y^*) \tag{16}$$

The heat balances in the gas and solid phases yield

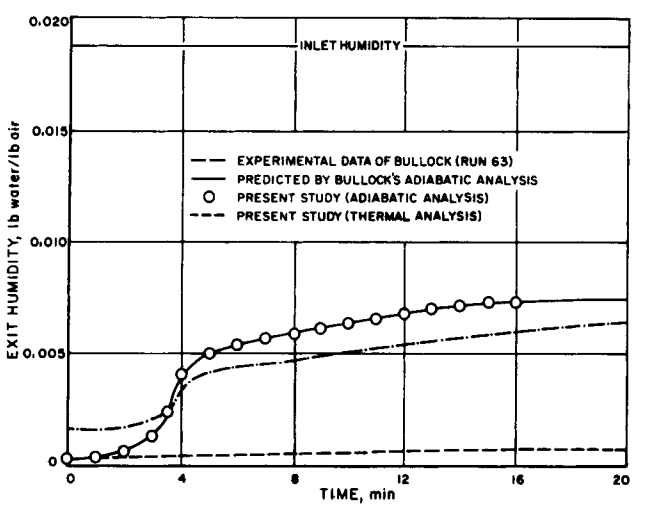

Fig. 6. Comparison of experimental and predicted exit humidity vs. time for silica gel (run 63).

$$\rho F\left(\frac{\partial H}{\partial t}\right)_x + G\left(\frac{\partial H}{\partial x}\right)_t = -\rho_s \left(\frac{\partial H_B}{\partial t}\right)_x \tag{17}$$

$$\rho_s \left(\frac{\partial H_B}{\partial t}\right)_x = h\, a_v (T - T^*) = K_Y\, a_v (Y - Y^*)\, H_g \tag{18}$$

The equilibrium humidity, Y^*, is a function of the amount of adsorbate in the adsorbent, w, and the temperature of the supporter on the adsorbent bed, T_B, that is,

$$Y^* = f(w, T_B) \tag{19}$$

The initial and boundary conditions are

$$w(x, t^0) = w^0 \tag{20}$$

$$H_B(x, t^0) = H_B{}^0 \tag{21}$$

$$Y(0, t) = Y_0 \tag{22}$$

$$H(0, t) = H_0 \tag{23}$$

Defining dimensionless variables n and τ by Equations (6) and (7) transforms $Y(x, t)$, $w(x, t)$, $H(x, t)$, and $H_B(x, t)$ into $Y(n, t)$ $w(n, t)$ $H(n, t)$, and $H_B(n, t)$ by application of chain differentiation. The resulting transformed equation may be written as follows:

$$\left(\frac{\partial Y}{\partial n}\right)_\tau = -(Y - Y^*) \tag{24}$$

$$\left(\frac{\partial w}{\partial t}\right)_n = \frac{1}{\alpha}(Y - Y^*) \tag{26}$$

$$\left(\frac{\partial H}{\partial t}\right)_\tau = -[N_{Le}(H - H^*) + (Y - Y^*)(H_g - 1060.91\, N_{Le})] \tag{26}$$

$$\left(\frac{\partial H_B}{\partial t}\right)_n = [N_{Le}(H - H^*) + (Y - Y^*)(H_g - 1060.01\, N_{Le})] \tag{27}$$

The generalized equilibrium relationship may be written as

$$Y^* = f(w, T_B) \tag{28}$$

with initial and boundary conditions

$$w(n, 0) = w^0 \tag{29}$$

$$H_B(n, 0) = H_B{}^0 \tag{30}$$

$$Y(0, \tau) = Y_0 \tag{31}$$

$$H(0, \tau) = H_0 \tag{32}$$

$$H_B = C_{p,s}(T - 32) + \alpha [H_a + w(H_L + \Delta H_R)] \tag{33}$$

$$N_{Le} = \frac{k}{hC_p} \tag{34}$$

Equations (24), (25), (26), and (27), the equilibrium relationship for any given adsorbent, (28), and the initial and boundary conditions given by Equations (29) through (32) were solved numerically on the digital computer employing the same technique described in the previous section.

The theoretical predictions of the present model were first checked by calculating several of Bullock's experimental data on silica gel. This was achieved by setting the weight fraction of salt impregnated on a supporter, α, equal to 1 in Equation (24) and the heat capacity of the solid adsorbent supporter, $C_{p,s}$, equal to zero in Equation (33).

The numerical solutions obtained for the general case are also applicable for the case of adiabatic adsorption in

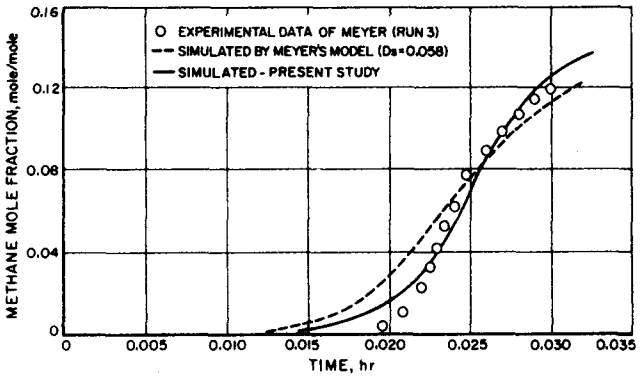

Fig. 7. Comparison of experimental and predicted exit methane concentration vs. time for activated carbon (run 3).

a single porous tube, provided n and τ are redefined by Equations (13) and (14).

EXPERIMENTAL PROCEDURE

Two methods are commonly employed to measure dynamic adsorption and desorption rates. One is to measure the inlet and effluent humidities of the stream by employing a hygrometer and the other is to weigh the adsorbent bed intermittently. In this study the latter technique was adopted because the time lag involved in weighing the adsorbent is virtually negligible.

Apparatus

The apparatus shown in Figure 2 was designed and constructed to study the effect of major variables such as inlet humidity, inlet temperature and mass velocity.

Measuring devices, recorders, and instruments to control flow, temperature, humidity, and weight were installed.

The following discussion gives the functions of each section of the apparatus and delineates those capabilities and limitations of the instruments that are critical to the experiment. For further details the reader is referred to elsewhere (9).

The compressed air contained excessive oil, dirt, and moisture, and required cleaning. The air was passed through two knockout drums in series and through a fine stone filter in the purification section.

The dehumidification and saturation section consists of two Gilbarco molecular sieve dryers (Model No. 200-120-058) to dry the air for reactivation and to regulate the humidity of the inlet stream by mixing it with saturated air, and a saturator with an isothermal bath. Temperature control is essential. The cleaned air was dried and/or humidified by regulating the relative flow rates with precision valves.

The prespecified inlet humidity was attained by mixing the dry and wet streams in a stainless steel tank. The resulting humidity was measured by a Gilbarco Hygrometer (Model SHL-100) and recorded on a Varian Model G-14A-1.

The desired temperature of the inlet stream was obtained by heating the air in a 9 kw.-capacity Chromalox circulating heater (Model CGH-6) controlled by a Chromalox industrial thermostat (Model AR-5519) and by a Fenwal precision temperature controller (Model 52-3XX2XX-XXX) that controls temperature to within ±1% of the desired range.

The heart of the apparatus is the test section shown in Figure 3. This apparatus was constructed with Kimax-tempered glass pipes which have metal joints and insulation; it consists of a weighing mechanism that includes a linear displacement transducer, a power supply, a calibrated spring, a transducer supporter, a center guide adjuster, two two-way ball valves, a test block holder, and a weight-change recorder. This is the section where the adsorption and desorption rates are measured.

Procedure for Adsorption-Desorption Rate Experiments

Sample Preparation. The 2 in. diameter by 1 in. length Torvex blocks were conditioned in an oven for a minimum of 12 hr. at 150°C. The block was weighed on an analytical balance and dipped into the desired salt solution. Excess solution was allowed to drip from the wet block. The salt-impregnated block was enclosed in a glass jar specially made for this purpose and placed in a vacuum oven overnight. The combined weight of the salt-impregnated test block and the glass was determined on an analytical balance. During weight measurement, the glass jar was kept closed to prevent adsorption of moisture by freshly regenerated adsorbent. Knowing the weight of the dry sample and the jar, the amount of salt impregnated was determined.

The test block thus prepared was placed in a thin-walled stainless steel cylindrical test block protector. The stainless steel center-guide rod was passed through the block and held to it by a nut.

Prior to the start of the experiments, the dryers ran for at least 24 hr. and the isothermal bath for the saturator was normally on for 4 hr. to reach steady state.

The zero point of the linear transducer reading—the combined weight of the anhydrous salt and the test block—was established before the start of each set of experiments by passing dry air heated to 240°F. through the test block for an hour or more and then equilibrating with extradry nitrogen having a moisture content of less than one ppm. To minimize the use of the extradry nitrogen the low pressure flow regulator Matheson Model 1260-3S was used. Because the system was heated to a high temperature to reactivate the adsorbent, and low flow rates were employed to conserve the extradry nitrogen, it generally took 24 hr. or more for the test block to equilibrate.

Adsorption. A small amount of cleaned air in accordance with the cleaning procedures of Figure 2, about 1,500 cc./min., was used to measure the inlet humidity. The upper ball valve was closed to maintain the equilibrated condition of the test block with dry nitrogen and the lower two-way ball valve was open to bleed the stream into the room when adjusting for humidity control. When desired inlet conditions were achieved and stabilized, the zero time was set simultaneously with the opening of the upper two-way ball valve and the closing of the other.

After a short period of time elapsed, usually a minute, the flow was reversed and the test block was released from the holder to measure the weight change of the block. To minimize the time required for the spring to reach its equilibrium displacement with the weight, very soft vibration was applied to the top of the spring holder with an engraver. As soon as the recording was complete, the block was set in place and the flow was switched back.

Every new adsorption experiment was started with the removal of moisture adsorbed in a previous run. This was accomplished by sending dry air heated to 240°F. through the wet test block for an hour or more, and equilibrating with liquid-pump dry nitrogen (humidity level of 17 to 20 ppm).

Desorption. In principle, cyclic adsorption-desorption rate experiments can be carried out, but the experiments were conducted separately.

The desorption rate experiment was carried out in a similar manner to that of the adsorption rate measurement except that the initial adsorbate content in the adsorbent was raised to a desired level by passing wet air through the bed, and the inlet temperature of the air was elevated.

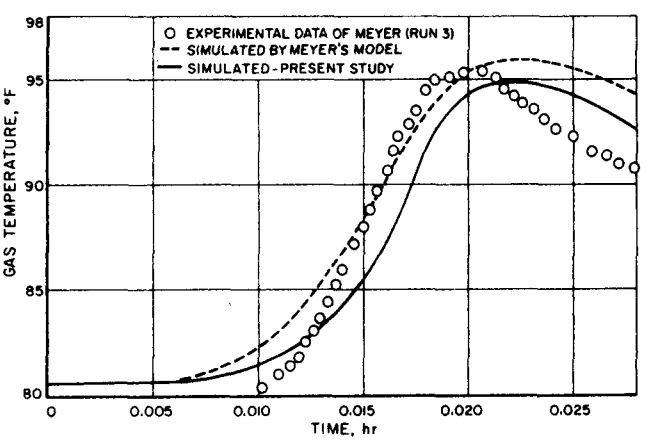

Fig. 8. Comparison of experimental and predicted temperature vs. time for activated carbon (run 3).

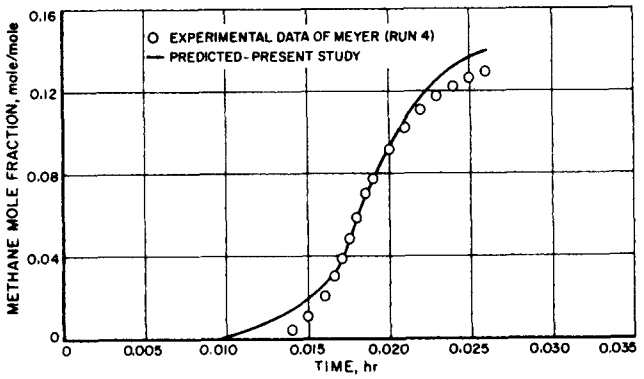

Fig. 9. Comparison of experimental and predicted exit methane concentration vs. time for activated carbon (run 4).

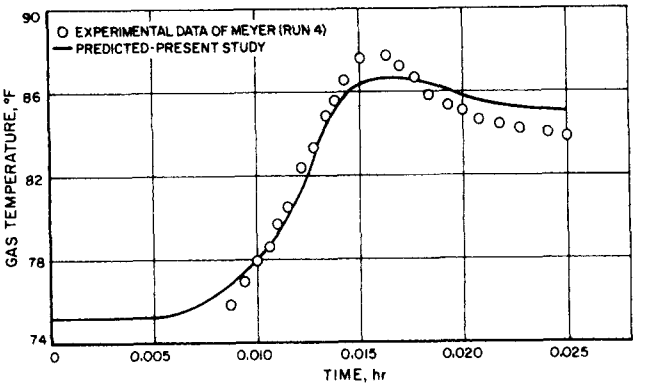

Fig. 10. Comparison of experimental and predicted temperature vs. time for activated carbon (run 4).

RESULTS AND DISCUSSION

Comparison of the Proposed Model with Published Experimental Data

The isothermal adsorption-desorption processes have not been well studied experimentally because of some of the inherent experimental difficulties generally encountered in maintaining isothermal conditions. Therefore, the proposed model for the isothermal adsorption process can not be directly verified. However, the literature data on the adsorption of water vapor from air by silica gel and on the adsorption of methane from helium by activated carbon are available to verify the proposed adiabatic adsorption-desorption model. The comparisons are presented below.

Air-Water-Silica Gel System

Three representative experimental runs (11, 12, and 63) of Bullock (*6*) for an unsupported adsorbent bed of silica gel were simulated on a digital computer with the models developed in the present study for isothermal and adiabatic dynamic adsorption-desorption processes.

Comparisons of the experimental and predicted humidities of the effluent stream plotted against time are presented Figures 4, 5, and 6. The heat and mass transfer coefficients and the Lewis number were determined from the empirical correlations for the adiabatic dynamic adsorption of water from humid air by silica gel presented by Hougen and Marshall (*17*). The equilibrium vapor pressure data used in obtaining the solutions were those reported by Hubard (*18*) and mathematically represented by Bullock.

Figure 4 compares Bullock's run 11. The agreement between Bullock s predictions and this study of the adiabatic adsorption process is quite satisfactory. The experimental data agree well with the adiabatic predictions during the initial period of the run, but, during the remainder of the run, the data fell between the adiabatic and isothermal predictions, indicating that a substantial amount of heat was lost during the experiment.

Figure 5 compares the results for run 12. The bed depth in this run was the same as in run 11 (1 in.), but the inlet air humidity and temperatures were lower. The experimental data fell closer to the results predicted by the isothermal analysis than to the prediction from the adiabatic analysis. This was expected from the results of run 11 because the lower inlet humidity would decrease the adsorption rate and lower the rate of heat release at a constant mass velocity.

Figure 6, which shows the results for a run that had the same inlet humidity as run 11 but had a deeper bed (6 in.) and a higher mass velocity, shows a sharp contrast to Figure 5. For deeper beds, maintaining a constant temperature in the gas stream flowing through a granular bed and undergoing adsorption becomes increasingly difficult because of the low thermal conductivity of the gas stream. Consequently, the experimental data closely follow the predictions of the adiabatic analysis.

In summary, Figures 4, 5, and 6, which show typical results for an unsupported adsorbent bed, illustrate the governing processes, that is, adiabatic or isothermal, the relative importance of the major variables, and the role of analysis which determines the upper and the lower bounds of the rate. The results of the proposed model are in excellent agreement with Bullock's prediction for the adiabatic adsorption of water vapor by an unsupported adsorbent bed; therefore, this comparison is believed to constitute a satisfactory test of the proposed generalized model for adiabatic adsorption. The discrepancies between the experimental data and the predictions of the adiabatic analysis may be attributed to the heat losses; to uncertainties in the equilibrium vapor pressure data, the heat of wetting data, and in determining the initial bed moisture content; and to simplifying assumptions made in the analysis.

Helium-Methane-Activated Carbon System

The adsorption rate data on the adsorption of methane by activated carbon recently reported by Meyer and Weber (*20, 21*) were analyzed next. Two experimental runs (3 and 4) for an unsupported adsorbent bed of Columbia SXC activated carbon were simulated on the computer.

Figures 7, 8, 9 and 10 show comparisons of the experimental and computed results of methane concentration in the effluent stream vs. time and the temperature-history of the gas phase at the three-quarter length of the adsorber. In this analysis, the effective heat and mass transfer coefficients were determined semi-empirically by comparing one set of experimental data (run 3) with the corresponding theoretical solutions. These coefficients were then employed to predict the rest of the data. The

Table 1. Summary of Runs for Adsorption and Desorption Rate Experiment

Test Block: Lithium Chloride Impregnated on Torvex

Run No.	Y_0, lb.water/ lb. air	T_0, °F.	Y_0, u, ft./min.	L, in.	α lb.salt/ lb. Torvex	W_0, lb.water/ lb. salt
707	0.015	90	300	1.0	0.03	0.10
713	0.015	110	300	1.0	0.03	0.10
807	0.010	150	300	1.0	0.03	2.0
808	0.010	200	300	1.0	0.03	2.0
805	0.001	150	300	1.0	0.03	2.0

TABLE 2. SOME PROPERTIES OF LiCl-H_2O-TORVEX SYSTEM

Weight of Torvex	17.1 g.
Ky	33.4 lb. H_2O/hr. sq.ft.—lb. H_2O/lb. air
a_v	384 sq.ft./cu.ft.
ρ_{Torvex}	40 lb./cu.ft.
$C_{p,LiCl}$	0.282 B.t.u./lb. °F.
$C_{p,Torvex}$	0.20 B.t.u./lb. °F.

equilibrium vapor pressure data used in theoretical computations were those reported by Meyer (*21*).

Figures 7 and 8 compare the results for run 3. Meyer determined the effective intraparticle diffusivity of 0.058 sq. ft./hr. The present authors determined the effective mass transfer coefficient of 2.7 lb. methane/hr./sq. ft.-lb. methane/lb. helium. The agreement between Meyer's simulated results and this study is satisfactory. Also, the experimental data for run 3 agree reasonably well with the computed results.

Figures 9 and 10 compare the results for run 4. The operating conditions of runs 3 and 4 were the same but the total pressure was changed from 99 to 64 lb./sq. in abs. The total pressure effects the capacity of the adsorbent and the lower pressure led to lower loading. Meyer could not predict the behavior of the adsorber (run 4) with the effective intraparticle diffusivity determined from the previous run. He therefore matched the observed and the computed effluent curves and found a different value for intraparticle diffusivity of 0.10 sq. ft./hr. for run 4.

The solid line in Figures 9 and 10 represents the predicted results of the present study for run 4 by employing the same transfer coefficients and the packing constant as determined in run 3. The experimental data agree reasonably well with the theoretical predictions. The deviations between the experimental data and the predictions of this study may be attributed (a) to uncertainties in the equilibrium vapor pressure data and in determining the initial bed moisture content, and (b) to simplifying assumptions made in the analysis.

The failure of Meyer-Weber's model to produce a consistent effective intraparticle diffusivity may be attributed to several factors: the model might not actually represent the physical process, the low accuracies of the transfer coefficients, and the truncation errors of the numerical solutions.

In summary, the validity of the Meyer-Weber model is yet to be established by a crucial test. The practical utility of their model is limited because of its severe restriction on the geometry of the adsorbents and its inability to predict the adsorber behavior of adsorbents impregnated on a supporter. Furthermore, in their study, they found that although the effective pore diffusivity is one of the most important parameters, its value is uncertain and the simulation of the experiments did not produce a consistent effective pore diffusivity.

The model proposed in this study is quite adequate for predicting the behavior of the adsorber, provided that the effective transfer coefficients are determined from the simulation of an actual experiment.

Comparison of the Proposed Model with the Present Experimental Data for the Lithium Chloride-Water-Torvex System

A total of 11 runs, of which five runs were desorption rate measurements, were made to determine the individual effects of the major variables as well as their combined effects. The details of these runs can be found elsewhere (*9*).

In this analysis the effective heat and mass transfer coefficients were determined from run 707. An effective mass transfer coefficient of 33.4 lb. water/hr. sq. ft.-lb. water/lb. air was used to predict the rest of the data for both adsorption and desorption experiments. The summary of the runs is presented in Table 1.

The effect of mass velocity on the mass transfer coefficient was determined from Hausen's empirical formula (*12*); it was found to be negligible over the range investigated in the present study. The literature equilibrium vapor pressure data (*3, 9, 15, 29, 31*) for unsupported lithium chloride-water system were used in obtaining the theoretical predictions, since it was found (*9*) that Torvex does not effect the vapor pressure of lithium chloride-water system. Some of the selected properties of this system are listed in Table 2.

Adsorption Data

Figures 11 and 12 compare the results for weight gain versus time and for the temperature history, respectively, for run 707. The solid line represents the results obtained by the adiabatic adsorption analysis compared with the experimental data. An excellent simulation was obtained.

Figure 13 illustrates the effect of inlet temperatures from 90 to 110°F. on the adsorption rate. The data agree with the theoretical predictions. As expected the adsorption rate decreased when the inlet temperature was raised. An increase in inlet temperature reduces the capacity of the adsorber substantially.

The effects of inlet humidity, mass velocity and the combined effects of these variables on the adsorption rate were also investigated. Again, in all these cases the theoretical model predicted the experimental data very well.

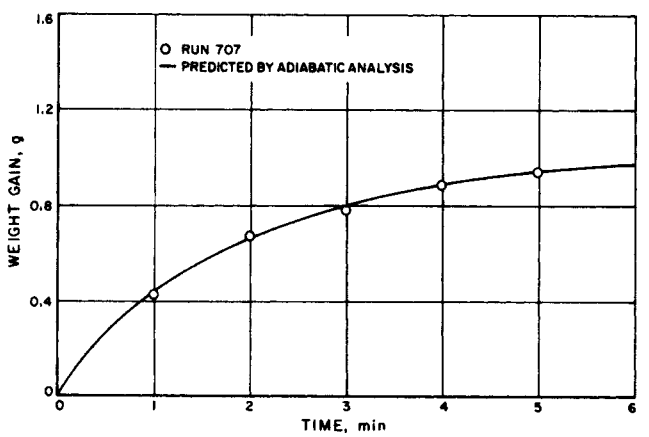

Fig. 11. Comparison of experimental and predicted weight gain vs. time (run 707).

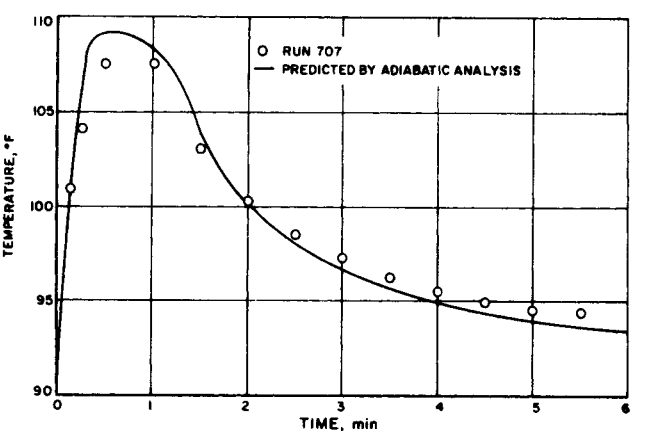

Fig. 12. Comparison of experimental and predicted exit temperature vs. time (run 707).

These comparisons can be readily found elsewhere (9).

Desorption Data

The desorption rate data obtained for the lithium chloride-water-Torvex system were also analyzed using the same transfer coefficients as determined from the adsorption rate experiment (run 707). Comparisons of the experimental data with the theoretical predictions for several of these desorption runs are shown in Figures 14 and 15.

Figure 14 illustrates the effect of inlet temperature on the adiabatic desorption rate. Run 807 may be used as a basis for comparison. The inlet temperature was increased from 150° (run 807) to 200°F. (run 808). The desorption rate increased considerably. A thorough regeneration of the adsorbent bed is possible only at a high temperature (for example 200°F.). The agreement between the experimental results for desorption and the theoretical predictions is satisfactory.

Figure 15 shows the effect of inlet humidity on adiabatic desorption rate. In this run the inlet humidity was reduced from 0.010 to 0.001 lb. water/lb. air. Its effect is similar to that of an increase in inlet temperature because both effects increase the concentration driving force and lead to a lower equilibrium loading. The experimental data agree well with the theoretical predictions.

The combined effects of the several independent variables that effect the desorption rate were also determined with good agreement between theory and data (9).

In general, the agreement between the present experimental data and the theoretical predictions is good within about ±10%. The sight discrepancies may be attributed to the following uncertainties: (a) in the vapor pressure relations used in obtaining the numerical solutions, (b) in determining the effective heat and mass transfer coefficients, (c) in the transfer area of the supporter, (d) in measuring the initial moisture content of the adsorbent and the temperature of the bed, and (e) in the simplifying assumptions (for example, that the heats of wetting and reaction remained constant, etc.). Also, in the adiabatic analysis it was assumed that there was no radial temperature gradient at the wall of the adsorbent bed, but in the experimental system, heat loss to the surrounding was inevitable. The effect of heat loss was probably quite small for most of the runs because the bed was shallow and the duration of the experiment was short. This is substantiated by the agreement between the experimental data and the predicted values. The discrepancies in the numerical solutions could have been introduced by

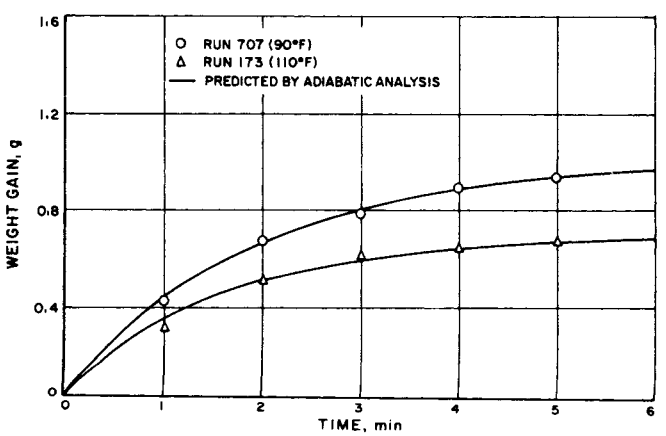

Fig. 13. Effect of inlet temperature on adiabatic adsorption rate and comparison of experimental and predicted weight gain vs. time (run 713).

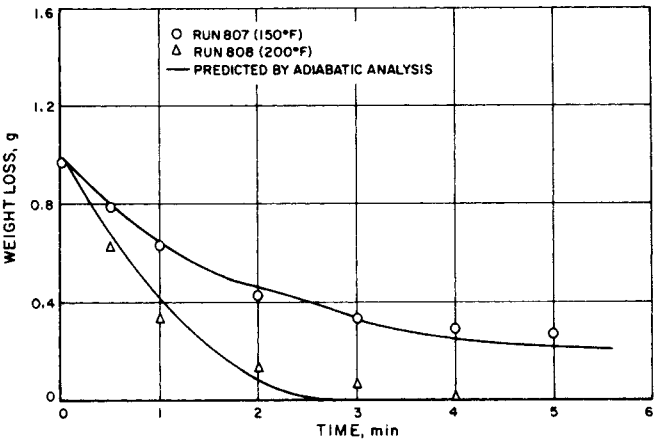

Fig. 14. Effect of inlet temperature on adiabatic desorption rate and comparison of experimental and predicted weight loss vs. time (runs 807 and 808).

uncertainties in the assumed operating conditions.

In an effort to further explain the deviations between the experimental data and the theoretical predictions, the effects of the parameters were determined quantitatively whenever possible. The effects of small deviations of the Lewis number, the initial bed temperature, and the initial moisture content of the adsorbent from the assumed values were studied and found to be negligible (9). Since a more sophisticated analysis would require excessive computer time, any additional effort to improve the accuracy of the models seems unjustifiable at the present time.

There are several limitations in the present model. The most serious limitation of the models is that they apply strictly to a single adsorbate component present in the gas phase. However, the general analytical approach developed in this study and the numerical technique used can be employed to the analysis of more complicated systems. Furthermore, this model has been satisfactorily tested only under the conditions where diffusion is the rate limiting step.

CONCLUSIONS

The mathematical models for a single adsorbate component present in a gas phase have been developed for isothermal and adiabatic dynamic adsorption-desorption processes with nonlinear equilibrium relationships. The proposed models describe, with sufficient accuracy, the design of unsupported fixed bed adsorbers.

The present models show considerable effects of supporters on the performance of both isothermal and adiabatic fixed beds of supported hygroscopic salts.

An experimental technique was developed to measure the adiabatic adsorption and desorption rates of water vapor by and from the hygroscopic salts impregnated on a supporter. The effects of major independent variables, temperature, humidity inlet stream and mass velocity, on the rates of adsorption and desorption have been determined experimentally. The experimental data were found to be in agreement with the proposed theory.

This type of analysis can be modified to include a mixed adsorbent bed and may be extended to types of engineering problems, such as regenerator, ion exchange and composite drying agents, molecular sieves, etc.

ACKNOWLEDGMENT

C. W. Chi gratefully acknowledges the financial support provided to him by the Institute of Gas Technology.

NOTATION

A = area
a_A = transfer area per unit superficial area
a_v = transfer area per unit volume
$C_{p,s}$ = heat capacity of solid/or adsorbent supporter
d = differential operator
F = porosity
f = function
G = mass velocity
H_a = enthalpy of adsorbent
H_B = enthalpy of adsorbent bed defined by Equation (33)
H_g = enthalpy of water vapor
H_L = enthalpy of liquid water
ΔH_R = enthalpy difference between the heat of adsorption and heat of normal condensation
H_s = enthalpy of adsorbent supporter
H^* = enthalpy of humid air at the surface of adsorbent
H_0 = enthalpy of inlet stream
$H_B{}^0$ = initial enthalpy of bed
h = heat transfer coefficient
K_Y = overall mass transfer coefficient
L = length of adsorbent bed
N_{Le} = Lewis number defined by Equation (34)
n = dimensionless bed length
R = radius
T = temperature of the gas
T_s = temperature of the solid
T^* = temperature of the adsorbent or adsorbent supporter
t = time
u = average linear velocity at the fluid
w = adsorbate content in the adsorbent
w^0 = initial adsorbate content in the adsorbent
x = axial distance
Y = humidity
Y_0 = inlet humidity
Y^* = equilibrium humidity at the surface of adsorbent

Greek Letters

α = ratio of salt weight to weight of supporter
ϵ = thickness of salt coating/tolerance in the program
ρ = density of air
ρ_a = bulk density of adsorbent
ρ_s = bulk density of solid or adsorbent supporter
ρ_s' = apparent density of adsorbent supporter
τ = dimensionless time

Superscript

* = equilibrium value
^{0} = initial condition

Subscript

a = adsorbent
A = area
B = bed
g = gas phase
s = solid phase, adsorbent supporter
w = water
x = cross section
0 = inlet condition

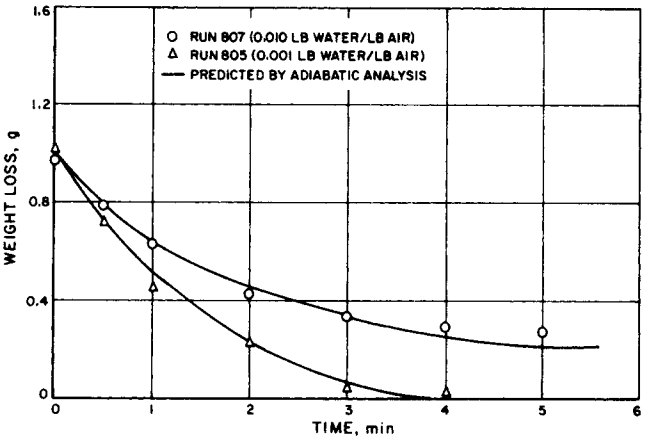

Fig. 15. Effect of inlet humidity on adiabatic desorption rate and comparison of experimental and predicted weight loss vs. time (run 805).

LITERATURE CITED

1. Acrivos, A., *Ind. Eng. Chem.*, **48**, 703 (1956).
2. Anzelius, A., *Z. Angew Math. Mech.*, **6**, 291 (1926).
3. Appleby, M. P., F. H. Crawford, and K. Gordon, *J. Chem. Soc.*, **11**, 19665 (1934).
4. Brand, L., "Advanced Calculus," John Wiley, New York (1955).
5. Brinkley, S. R., Jr., *J. Applied Phys.*, **18**, 582 (1947).
6. Bullock, C. E., Ph.D. thesis, Univ. Minnesota, (1965).
7. ———, and J. L. Threlkeld, Preprint for inclusion *ASHRAE Trans.* (Feb. 1966).
8. Carter, J. W., *Trans. Inst. Chem. Engrs.*, **44**, T253 (1966).
9. Chi, C. W., Ph.D. thesis, Illinois Inst. Tech., Chicago (Jan. 1968).
10. Collins, J. J., *Chem. Eng. Progr. Symposium Ser. No. 74*, **6**, 31 (1967).
11. Eagleton, L. C., and H. Bliss, *Chem. Eng. Progr.*, **49**, 543 (1953).
12. Eckert, R. R. G., and R. M. Drake, Jr., *Heat Mass Transfer* **198**, 504 (1959).
13. Fosberg, T. M., and C. E. Phillips, presented at the AIChE Meeting, Salt Lake City, Utah, (May, 1967).
14. Gamson, B. W., G. Thodos and O. A. Hougen, *AIChE Trans.*, **39**, 1 (1943).
15. Gocken, N. A., *J. Amer. Chem. Soc.*, **73**, 3789 (1951).
16. Hausen, H., *Tech. Mech. Thermodynam.*, **1**, 219 (1930).
17. Hougen, O. A., and W. R. Marshall Jr., *Chem. Engr. Progr.*, **43**, 197 (1947).
18. Hubard, S., *Ind. Eng. Chem.*, **46**, 356 (1954).
19. Lee, H., and W. P. Cummings, *Chem. Eng. Progr. Symposium Ser. No. 74*, **63**, 42 (1967).
20. Meyer, O. A., and T. W. Webber, *AIChE J.*, **13**, 457 (1967).
21. ———, Ph.D. thesis, State Univ. New York at Buffalo, (1966).
22. Michaels, A. S., *Ind. Eng. Chem.*, **44**, 1922 (1952).
23. Milne, W. E., "Numerical Solution of Differential Equations," John Wiley, New York (1953).
24. Nusselt, W., *Z. Ver. deut. Ing.*, **71**, 85 (1927).
25. Punwani, D., M.S. thesis, Illinois Inst. Tech., Chicago (Jan. 1967).
26. Rosen, J. B., *J. Chem. Phys.*, **20**, 387 (1952).
27. ———, *Ind. Eng. Chem.*, **46**, 1590 (1954).
28. Schumann, T. E. W., *J. Franklin Inst.*, **208**, 405 (1929).
29. Slonim, C. H., and G. F. Huttig, *Z. Physik. Chem.*, **141**, 55 (1929).
30. Testin, R. F. and Stuart, E. B., *Chem. Eng. Progr. Symposium Ser. No. 74*, **63**, 10 (1967).
31. Thakker, M., M.S. thesis, Illinois Inst. Tech. (Jan. 1967).
32. Thomas, H. C., *J. Amer. Chem. Soc.*, **66**, 19664 (1944).
33. Threlkeld, J. L., "Thermal Environmental Engineering," p. 288, Prentice-Hall, Englewood Cliffs, N. J. (1962).
34. Tien, C. and G. Thodos, *AIChE J.*, **5**, 373 (1959).
35. Treybal, R. E., "Mass Transfer Operations," p. 504, McGraw-Hill, New York (1955).
36. Van Arsdel, W. B., *Chem. Eng. Progr. Symposium Ser. No. 16*, **51**, 47 (1955).
37. Vermeulen, T., and N. K. Hiester, *J. Chem. Phys.*, **22**, 96 (1954).
38. ———, *Advan. Chem. Eng.*, **2**, 147 (1958).

Manuscript received March 13, 1968; revision received June 24, 1968; paper accepted July 18, 1968. Paper presented at AIChE Los Angeles meeting.